A review of momentum models for the actuator disk in yaw

Hur, Chihoon; Berdowski, Tom; Ferreira, Carlos; Schepers, G.; Boorsma, K

DOI
10.2514/6.2019-1799

Publication date
2019

Document Version
Final published version

Published in
AIAA Scitech 2019 Forum

AIAA SciTech Forum
7-11 January 2019, San Diego, California
AIAA Scitech 2019 Forum

10.2514/6.2019-1799

Check for updates

A review of momentum models for the actuator disk in yaw

C Hur[1], T Berdowski[2], and C Ferreira [3]
Wind Energy Section, Faculty of Aerospace Engineering, Delft University of Technology, 2629 HS Delft, The Netherlands

and
G Schepers [4], K Boorsma [5]
Netherlands Organisation for Applied Scientific Research (ECN part of TNO), 1755 LE Petten, The Netherlands

BEM (Bladed Element Momentum) models have shown to be inaccurate in predicting loads in the case of yawed flow [1-3]. Actuator disk momentum theory is the basis for BEM codes, following Glauert's auto-gyro theory [4]. Therefore, a first step to improve BEM in yawed flow is to assess momentum models for the actuator disk in yaw and investigate possibilities for improvement. In the past, several models have been developed for an actuator disc under yawed conditions, but they are subject to various assumptions. In this paper, different yaw models for the actuator disk will be reviewed and compared against higher fidelity models: fixed and free [5] wake vortex models so that the earlier made assumptions can be assessed. The comparison considers the case of a uniformly loaded actuator disk at varying yaw angle (0°~90°) and thrust coefficient (0.1~0.9). From the models which have been assessed, Øye's correction [6] performs best, however, this model too suffers from deficiencies. This indicates that an improved momentum model for yawed flow is necessary.

I. Nomenclature

ε	= Relative ratio of induction field
Γ	= Circulation of vortex
Φ_y, Φ_z	= Yaw angle, azimuthal angle
a_x, a_y, a_z, a_n	= Induction factors on x axis, y axis, z axis and direction normal to the disk
f_d	= Force normal to the disk
x, y, z(Cartesian coordinate)	= x is on axial direction aligned with free stream velocity
C_P , C_T	= Power coefficient, thrust coefficient
D, R, r	= Diameter of disk, Radius of disk, radial position along the disk
F_r	= Radial dependency function
K_x	= K function as skewed angle
P, P_0	= Power, Power at non-yawed flow
U_∞	= Free stream velocity
$U_{i,total}$, $U_{i,average}$, $U_{i,inclined}$	= Resultant, average, inclined induced velocity normal to the disk
X	= Skewed angle

II. Introduction

Wind turbines in atmospheric conditions are continuously exposed to yaw misalignment due to the fact that the yaw control cannot follow the wind direction fluctuation instantaneously or due to the failure of the yaw control. Yaw leads to a very complex flow field in the rotor and in the wake of Horizontal Axis Wind Turbines (HAWT) [7]. The most widely used method for designing wind turbines is the Blade Element Theory (BEM) theory due to its

---

[1] PhD candidate, Delft University of Technology
[2] PhD candidate, Delft University of Technology
[3] Associate Professor, Delft University of Technology
[4] Senior Scientist Specialist, *ECN part of TNO*
[5] Senior Scientist Specialist, *ECN part of TNO*

computational efficiency. This theory is computationally efficient, which is a basic requirement for wind turbine calculations on the design process [7]. The BEM model is a combination of the momentum theory which considers the conservation of momentum on a stream tube surrounding an actuator disc representing the rotor, and the blade element theory which describes the local flow field around an airfoil. The basic BEM model has been derived for non-yawed conditions, but the BEM models implemented in design codes apply engineering models to overcome this assumption [7]. However, such engineering models have shown to be inaccurate in predicting loads in the case of yawed flow [1-3].

The main focal point for the engineering methods at yawed conditions lies on the modelling of the flow field in the rotor, i.e the modelling of the induced velocities in the rotor plane. These induced velocities are basically found in two steps: a rotor averaged value is found from the thrust coefficient with the actuator disk momentum theory following Glauert's auto-gyro theory [4]; on top of that a variation of the induced velocity in the actuator disc is modelled using several corrections have been invented under a large number of assumptions [6, 8-10]. The variation of induced velocities is often modelled as a sinusoidal variation with azimuth angle where the amplitude of the variation increases linearly with radial position. The many assumptions made in the derivation of the resulting yaw model and the questions how these assumptions affect the performance of the models form the motivation for this research. We aim to answer this question with higher fidelity models, i.e. frozen and free wake vortex methods [5]. Such methods model the flow physics, and in particular the induced velocities at yawed conditions in a very realistic way [11] and which nowadays can be applied at practical computational efforts. Thereto the results from the engineering yaw models are compared with results from higher fidelity models for the very basic starting point of every BEM model: a uniformly loaded actuator disc, which in the present study is not only modelled in aligned flow but also at yaw angles varying from 0 ~ 90° with changing thrust coefficient from 0.1 to 0.9.

In chapter III current yaw models and their assumptions will be reviewed. In Chapter IV some cases, using different yaw models will be selected and analyzed among 90 cases, using different yaw models to validate current yaw models. In chapter V, the conclusions of this review paper will be made, where current engineering yaw models are accurate enough or if there is a need for improvement.

III. Description of the models

In this chapter current moment yaw models for yawed conditions and higher fidelity vortex models will be explained.

A. Glauert's modified momentum theory

Prandtl [12] suggested a lifting-line model, assuming an uniform induced velocity which is caused by trailing vortices along the blades. Based on his model, Glauert [4] has proposed the modified momentum balance as Eq. (1) for a helicopter flying forward, which to some extent is similar to a wind turbine in yawed flow (Please refer to Fig. 1 for the concept of Glauert's yaw model.). The details of the derivation are well described in Burton's text book [13].

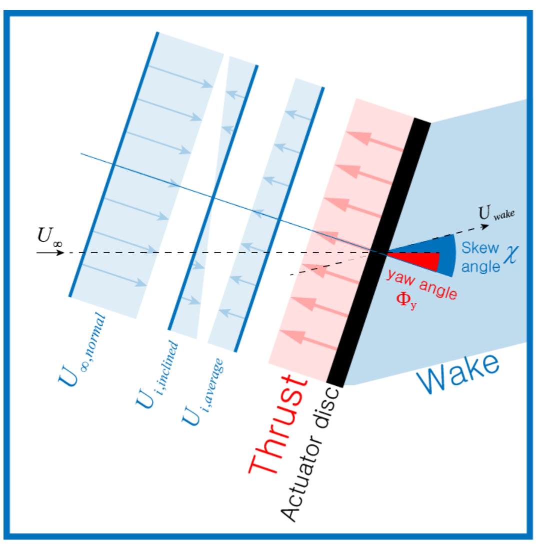

Fig. 1. The concept of Glauert's yaw model

$$C_T = 4a_n\sqrt{1-a_n\left(2\cos\Phi_y - a_n\right)} \tag{1}$$

Where the induction factor normal to the disk, a_n is ($U_{i,average}$ + $U_{i,inclined}$)/ U_∞. Therefore the relation between the C_T and the a_n depends on yaw angle. The average induced velocity, $U_{i.average}$, is assumed to be uniform on the actuator disk. On the top of that the non-uniformity of induction field caused by the skewed wake is proposed by Glauert as below Eq. (2).

$$U_{i,total} = U_{i,average} + U_{i,inclined} = U_{i,average}\left(1 + K_x \frac{r}{R}\sin\Phi_z\right) \tag{2}$$

Glauert suggested a constant value 1.2 for K_x [14] which describes the non-uniformity of the induction field at the disk in yawed flow. As shown in Fig. 1, on top of average induced velocity, $U_{i.average}$, the induced velocity, $U_{i,inclined} = U_{i,average}K_x r / R\sin\Phi_z$, is additional induced velocity caused by skewed wake effects, which is linear due to the constant K_x in momentum yaw models. Therefore the total induced velocity varies linearly with radius and sinusoidally with azimuthal angle Φ_z with constant K_x. Therefore the resultant induced velocity $U_{i,total}$ consists of average induced velocity $U_{i,avg}$ and inclined induced velocity $U_{i,inc}$ as described in Fig. 1 Some more attempts have been made to estimate K_x more accurately, considering the effects of the skewed angle in the rotor plane. The skewed angle is determined in several references [6, 13, 15] based on velocity components at rotor. While in the literature skewed angle is assumed to be constant in streamwise direction along the wake, Jiménez [16] suggested a skewed angle which changes along the wake based on the momentum conservation on lateral direction (y axis) as below Eq. (3).

$$X_{x=0} \approx \cos^2\Phi_y \sin\Phi_y \frac{C_T}{2} + \Phi_y \tag{3}$$

Where the $X_{x=0}$ is the skewed angle at the rotor.

$$X_{x\neq 0} = \frac{\cos^2\Phi_y \sin\Phi_y \frac{C_T}{2}}{1+\beta\frac{x}{D}} + \Phi_y \tag{4}$$

Where the $X_{x\neq 0}$ is the skewed angle along the wake. In his paper, the dependency on X is reflected through β which has been tuned with LES calculations at different yaw angles and thrust coefficients. It is found that reasonable β value ranges between 0.09 and 0.125 [16]. Due to its more physical description of the wake geometry, Jiménez's model for the skewed angle will be applied in this paper. For momentum models and the prescribed wake vortex model the skewed angle is assumed to be constant, using Eq. (3). And In the free wake vortex model the skewed angle will differ along the wake according to Eq. (4).

1. Coleman's model (1945)

Under the assumption that vorticity is created at the edge of the rotor only and then convected into the wake, where moreover the wake expansion is neglected and an infinite number of blades is assumed with constant circulation on the blades, Coleman [8] developed a simplified vortex model for a helicopter in forward flight. He derived the induced velocity along the diameter where z = 0 in a closed form solution as a function of the geometry of vortex rings on azimuthal component (y-z plane) and the strength of vortex. The induced velocity was obtained by the integration of Biot-Savart low from the assumed vortex cylinder wake leading to:

$$K_x = \tan\frac{X}{2} \tag{5}$$

2. White and Blake's model (1979)

White and Blake [10] developed an analytical model by combining prescribed lifting line theory with simple classical rotor equations. The simple model was correlated with measurements and predicted the non-uniform induced velocity caused by the skewed wake as Eq. (6) below.

$$K_x = \sqrt{2}\sin(X) \tag{6}$$

3. Pitt and Peters' model (1980)

Pitt and Peters [9] developed a linear and unsteady model to find the relation between the dynamic loads and the induction factor on the disk. The actuator disk theory in literature [17] is based on acceleration potential function which satisfies the Laplace equation. Based on the unsteady model Pitt and Peters also suggested an analytical solution for the induced velocity which varies linearly with the skewed angle as equation Eq. (7) below.

$$K_x = \frac{15}{32}\tan\left(\frac{X}{2}\right) \tag{7}$$

4. Øye' model (1992)

Ø ye [6] developed a model for the induced velocity distribution based on an actuator vortex ring model of wind turbines under the same assumptions as made in the derivation of Coleman's model [8].

$$U_{i,total} = U_{i,avg}\left(1 + F_r K_x \sin\Phi_z\right) \tag{8}$$

Here the K_x is tan(X/2) which is same as used in Coleman's yaw model. Unlike Coleman's correction Ø ye added a non-linear radial dependency, F_r, on the slope of the induced velocity approximation as below Eq. (9).

$$F_r = \left(\frac{r}{R}\right)^2 + 0.4\left(\frac{r}{R}\right)^4 + 0.4\left(\frac{r}{R}\right)^6 \tag{9}$$

5. Other related yaw corrections

Schepers' model (1999)

Based on the measurement Schepers [18] suggested a new yaw model, using Fourier series expansions. This model is able to predict the root vortex effects, while other momentum models implicitly consider tip vortex effects only. Since this model aims at predicting root vortex, this model won't be treated in this paper since the subject of the present paper is on momentum yaw models which consider the effects caused by tip vortex only.

Branlard's model (2014)

By extending Coleman's yaw model [8], an engineering yaw model has been suggested by Branlard recently to derive all components of the induced velocity. Using the superposition of skewed vortex cylinders, not only vorticity on azimuthal direction but also vorticity on longitudinal direction can be assessed including the root and bound vortex. The swirl in the wake caused by the finite tip speed ratio can be expressed as the vortex on longitudinal direction. Also the trailing vortex caused by non-uniform bound circulation can be described in his model [19]. Therefore the assumption of infinite tip speed ratio and constant bound circulation as present yaw momentum models can be relaxed. Since the model has the same approach to obtain induced velocity normal to the disk as Coleman's yaw model, this model is not dealt with in the paper.

B. Vortex wake models

1. Prescribed (Frozen) wake vortex model

A 3 dimensional (3D) prescribed wake vortex ring model has been developed, neglecting wake expansion, and assuming a uniform load at the disk. The assumption of uniform load at the disk makes that the vortices are created at the edge of disk only. In this case the strength of vortices can be derived as Eq. (10) [20].

$$\frac{D\Gamma}{Dt} = C_T \frac{1}{2} U_\infty^2 \tag{10}$$

Where Γ is the strength of vortex and t is time. At the edge of the actuator disk vorticity will be created with the strength as Eq. (10), and will be convected downstream on the surface of vortex cylinder with constant speed U_∞(1-a). Then due to the lateral force from the actuator disk to inflow the vorticity will be deflected with the skewed angle as defined in Eq. (3). Since the skewed angle is assumed constant in this model, vorticity exist on azimuthal direction only.

2. Free wake vortex ring models

Additionally, a free wake vortex ring model was developed by Berdowski [5] and used for validating momentum models. This model has been validated by comparing model results with wind tunnel and numerical results from literature.

Based on the wake geometry and the strength of vortex models, the induction field normal to the disk can be obtained by Biot-Savart law. To deal with the singularity of the vorticity, the induced velocity is multiplied with a Gaussian core. Note that the core size of the free wake model in this paper is 12.5 % of the disk diameter for the better convergence of the simulations at higher C_T, where the core size of the prescribed wake model is 2.5 % of the disk diameter of disk for all cases. Because at higher C_T the flow becomes so turbulent that the wake expansion is not well developed and the density of vorticity is higher in near wake, the validity of the free wake vortex model decreases. The validity of the free wake vortex model at high C_T will be treated in the section IV.B.1.

IV. Case studies

Both the 3D induction field and the induction field normal to the disk have been compared, using different momentum and vortex models at different values of C_T (0.1 ~ 0.9 with step of 0.1) and yaw angles (0 ~ 90 deg with step of 10 deg). Due to the advanced physical representation of the free wake vortex model, it is regarded as the most accurate model in this paper. Hence, the results calculated by four yaw momentum models and the prescribed wake vortex model will be compared with free wake and will be analysed. The thrust on the disk assumed uniform on the disk. Therefore 90 cases are calculated, several of them are selected for the purposes as shown in the table 1.

A. Operational conditions and comparison cases

The simulation cases are divided into four categories as seen in Table 1. Firstly Case I has been carried out to validate the free wake vortex model for non-yawed cases. Secondly induction fields have been analysed to check the dependency of C_T in Case II. Thirdly yaw angle dependency has been studied in Case III. Lastly, thrust and power coefficient in yawed conditions has been analysed in Case IV.

Table 1. Cases for comparison with different C_T and yaw angle

	Case I	Case II	Case III	Case IV
C_T	0.1, 0.6, 0.9	0.1, 0.3, 0.6	0.6	0.6
Yaw angle	0 deg	30 deg	10, 60, 90 deg	30 deg
Purpose	Model validations for Non-yawed flow	Investigation of C_T dependency at fixed yaw angle	Investigation of yaw angle dependency at fixed C_T	Prediction of C_T and C_P based on induced velocity a_n

B. Comparisons of yaw models

1. Case I: Non-yawed cases

For non-yawed inflow, all the momentum models have the same induction field. However, the results from vortex models find a non-uniformity of the induction field at the edge of the disk due to the radial velocity which is not modelled by the momentum methods. This non-uniformity is explained well in Sørensen's text book [21]. Also Kuik [22] proves that the absolute velocity at the rotor is constant. Furthermore it is important to consider the radial velocity in the model, especially for yawed conditions, which will be explained in the section IV.B.2-3 .

The average induction fields from all models matches well, while at higher C_T the induction factor of the free wake model is lower as described in figure 2. The reason is regarded as that the flow becomes more turbulent, violating the assumption of inviscid flow, resulting in shorter wakes. The validity of the induction field from vortex models at the very edge of disk is questionable due to the singularity of the vorticity and the core size as mentioned in the section III.B.2.

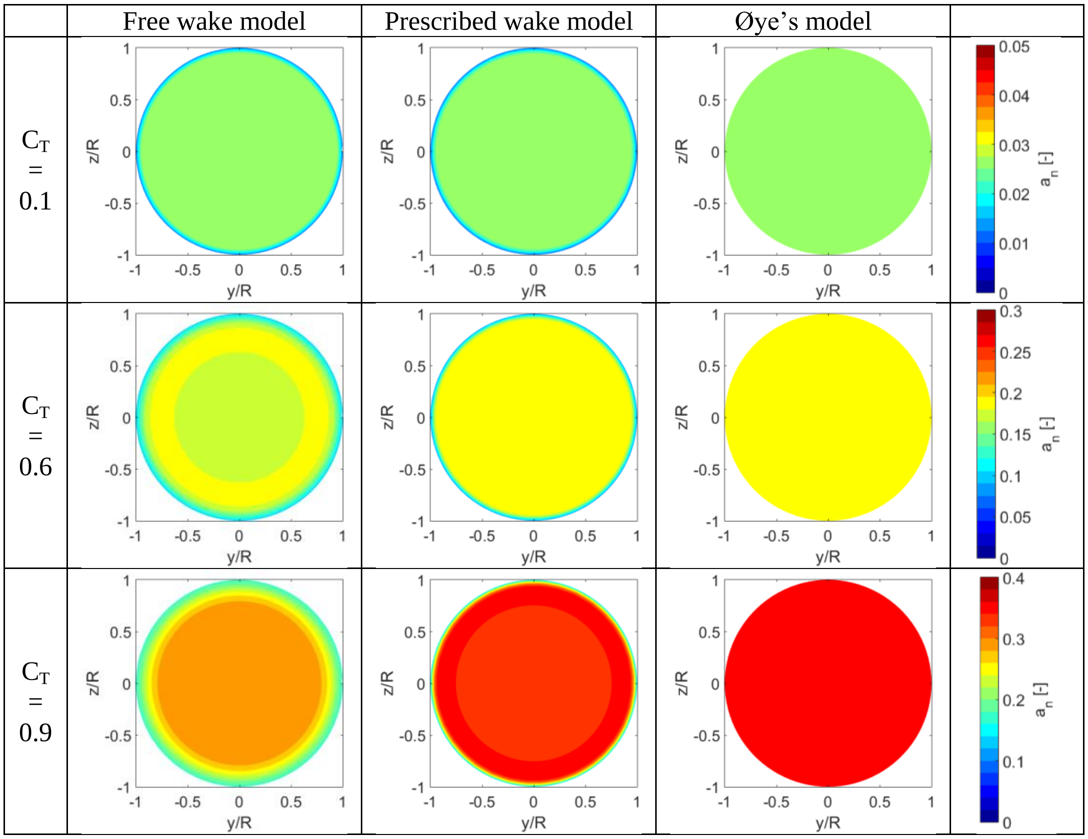

Fig. 2. Induction field (a_n) of Case I (yaw angle = 0 deg)

Momentum theory breaks down for a highly loaded actuator disk. To overcome the breakdown of momentum theory Glauert [23] suggested an experimental momentum relation for a highly loaded disk as described in Fig. 1. The induced velocity at the centre of the disk (z/R = 0, y/R = 0) from different models is compared to check the validity of the free wake vortex model. At C_T = 0.6, the relative deviation of induction factor at the centre of disk is approximately 3%, which is acceptable. Therefore the results of the free wake vortex model from C_T = 0.1 to C_T = 0.6 will be used in sections IV.B.2-3.

Glauert's experimental momentum relation in Fig. 1 has until now only been verified at non-yawed conditions. The detailed research for a heavily loaded disk in yaw is recommended to be carried out in the future.

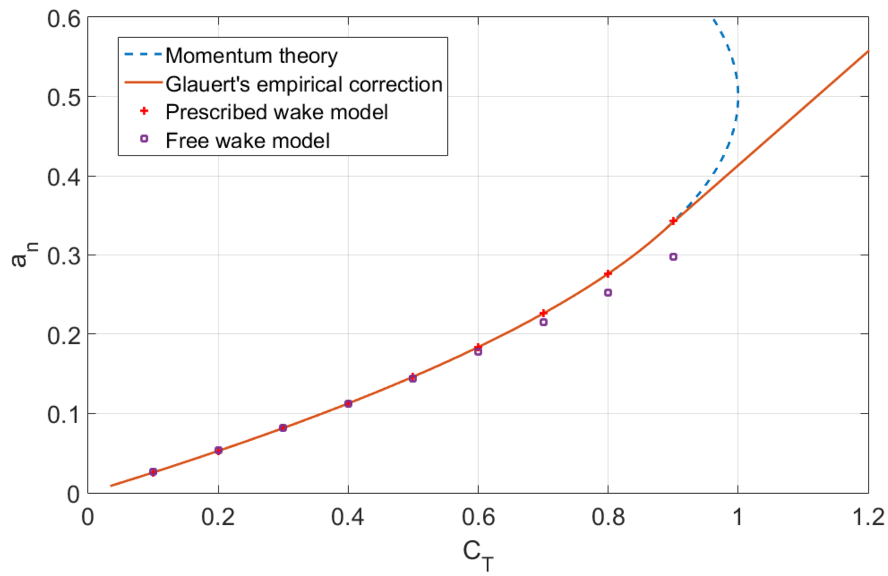

Fig. 3. Comparison of momentum balance at the point where z/R = 0, y/R = 0 and yaw angle = 0 deg

2. Case II: C_T dependency (0.1, 0.3, 0.6) at yaw angle = 30 deg

Fig. 4 shows the induction field normal to the disk calculated from momentum models and vortex models. Results fluctuate depend on yaw models and C_T. In general the Coleman's model underestimates the variation of the induction field, and Pitt and Peter's model overestimates the variation of induction field compared to results from vortex models. Øye's model agrees well with the results from the prescribed vortex model. The reason is expected to be that both models are based on a similar prescribed wake vortex ring approach using the same assumptions. Also Coleman and Øye's correction are based on the same prescribed vortex wake model, but Øye's model applied a non-linear radial dependency, showing a better accuracy.

Fig. 5 describes the relative ratio ($\varepsilon = \frac{a_n(momentum\ models) - a_n(free\ wake\ model)}{a_n(free\ wake\ model)} \times 100$) of induction field normal to the disk based on the free wake vortex model At lower C_T the skewed angle is smaller according to Eq. (3), resulting in less variation of the induction field compared with higher C_T cases. At higher Ct, Coleman's and Øye's model matches well with the free wake vortex model. However, Coleman's model has a poor prediction at the outer part of disk since it does not describe the non-linearity. Øye's model has mirror symmetric induction field on z axis, showing un-accurate induction file at the outer part of disk, especially it underestimates induction field in the downwind part (y/R > 0 & y/R < 1) as shown in Fig. 5.

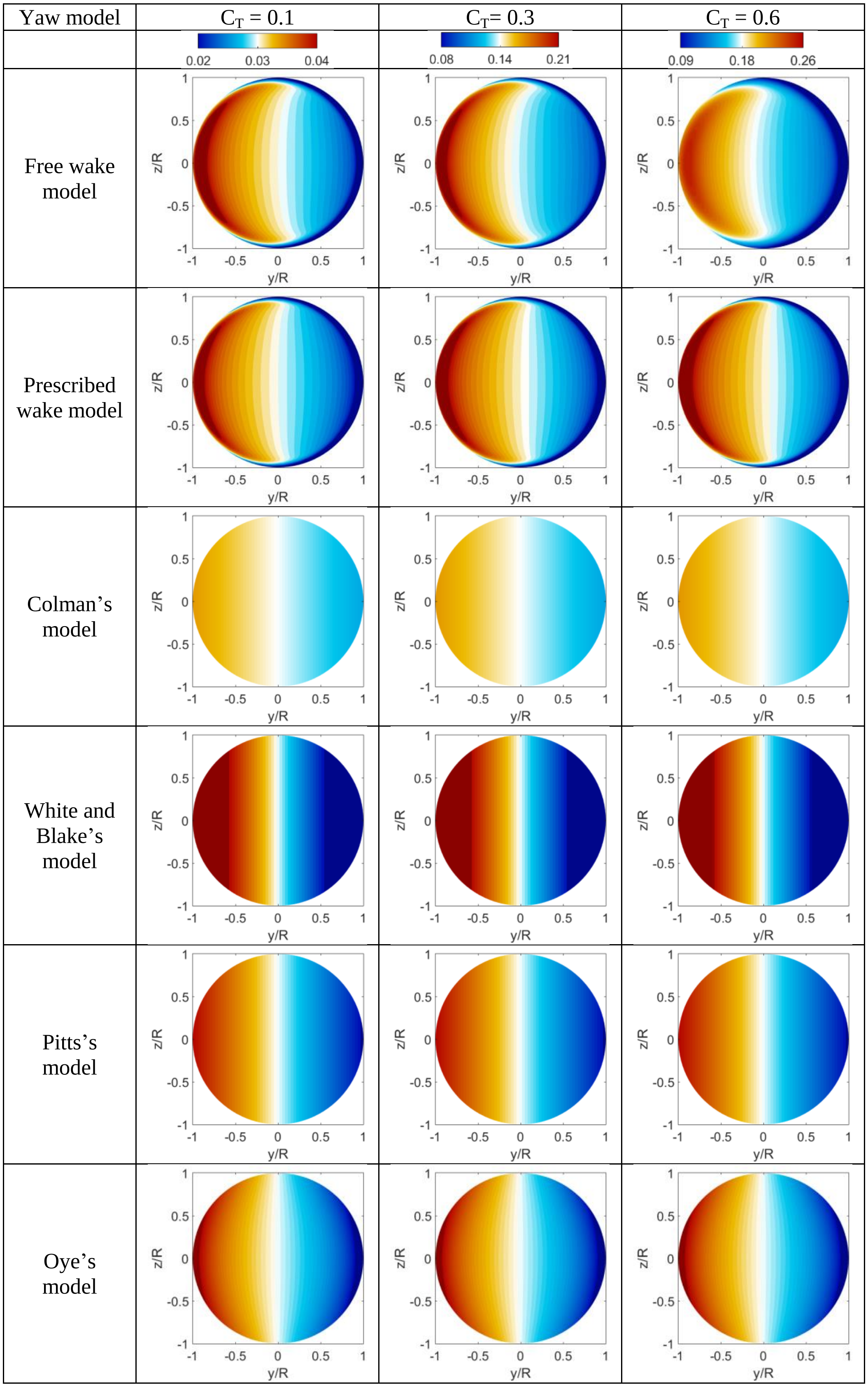

Fig. 4. Induction field (a_n) of CASE II (C_T = 0.1/0.3/0.6, yaw angle = 30 deg)

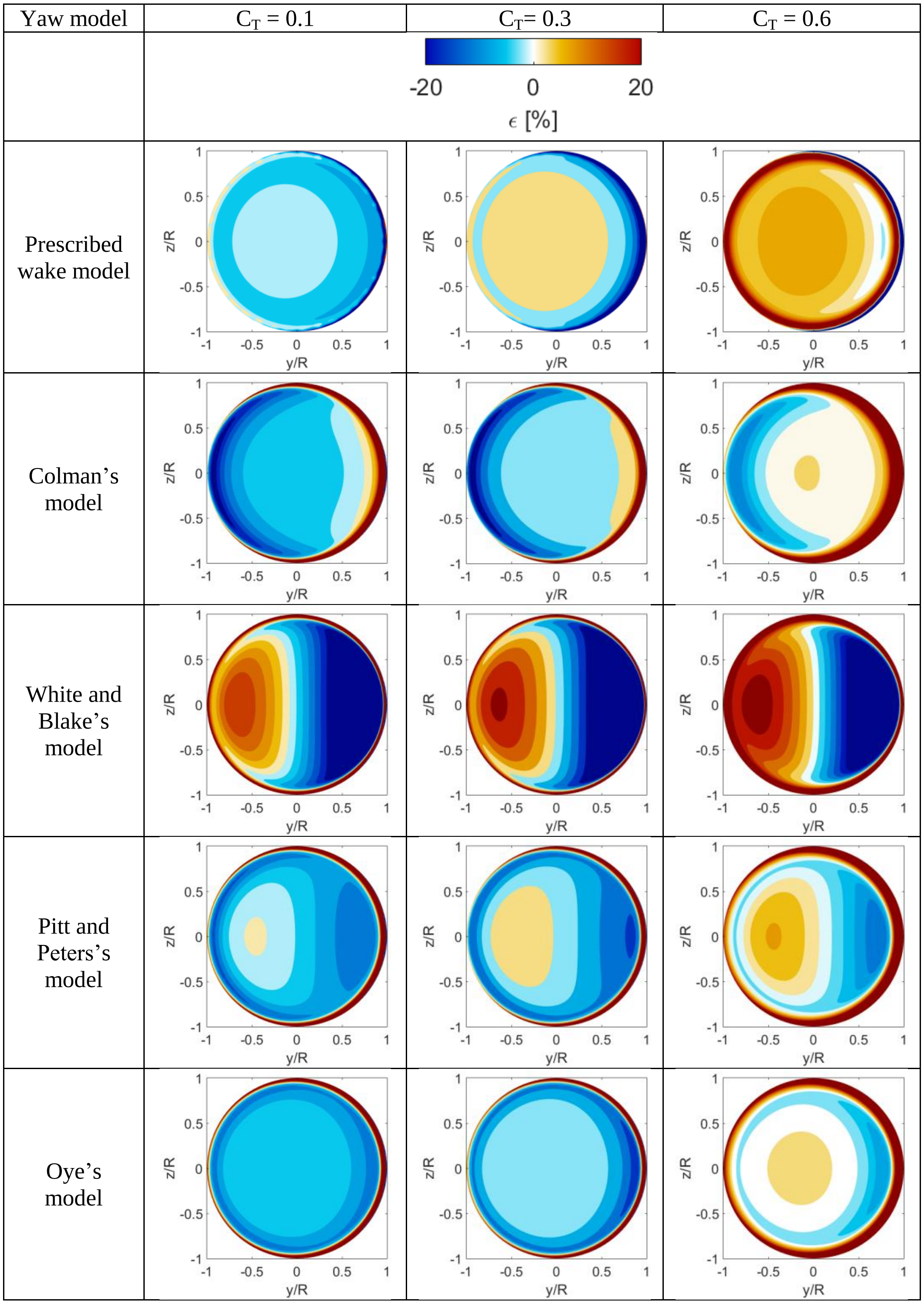

Fig. 5. Relative ratio of induction field (ε) of CASE II (C_T = 0.1/0.3/0.6, yaw angle = 30 deg)

In Fig. 6. 3-dimentional induction field (a_x, a_y, a_z) and induction field normal to disk (a_n) (z/R = 0, C_T = 0.6, yaw angle = 30 deg) from the vortex models are expressed along the radial distance non-dimensionalised with disk diameter where the z/R is 0. Therefore, a_x, a_y and a_z represents induced axial, radial and azimuthal velocity respectively (where the incoming velocity is assumed to be 1 m/s). The induced axial velocity in downwind part (y/R > -1 & y/R < 0) is slightly higher than the upwind part (y/R > 0 & y/R < 1), while the induced radial velocity increase significantly at the edge of the disk due to the vortices on azimuthal direction. Since the induced radial velocity (a_y) on the upwind part contributes a negative induced velocity normal to the disk (a_n), the induction field normal to the disk decreases. On the other hand, since the induced radial velocity (a_y) in the downwind part contributes a positive induced velocity normal to the disk, this effect leads to an increase in induction field normal the disk (a_n). This increases $da_n/d_{y/R}$ as shown in Fig. 6. Micallef [24] also proved that radial velocity increases dramatically in yawed flow for horizontal axis wind turbines. This higher induced radial velocity, gives induction field normal to the disk a much higher slope of the induction field. Sorenson [25] also proves that the higher thrust coefficient on the disk in yaw increases the radial velocity.

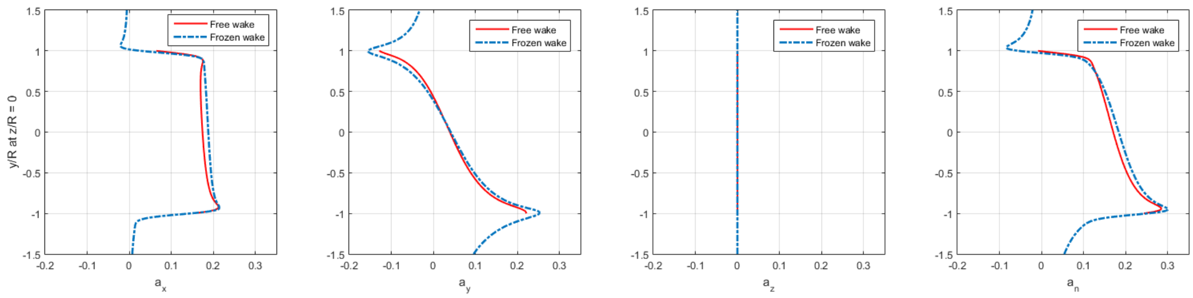

Fig. 6. 3-dimentional induction field (a_x, a_y, a_z) and induction field normal to disk (a_n) (z/R = 0, C_T = 0.6, yaw angle = 30 deg)

The prescribed vortex model overestimates the variation of radial velocity a_y and the reason is regarded as it cannot depict the wake expansion. Without wake expansion, the vorticity of the prescribed wake vortex model behind the rotor is closer to the disk than the free wake vortex model. (Please refer Fig. 9 describing the wake geometry of two vortex models.) Therefore the validity of prescribed vortex approach decreases because of neglecting wake expansion. It can be concluded that the radial velocity plays an important role for predicting the load normal to the actuator disk in yawed conditions, especially for higher thrust coefficients.

3. Case III: Yaw angle dependency at C_T = 0.6

Fig. 7 shows induction fields normal the disk with different yaw angels (yaw angle = 10/60/90 deg) and constant thrust coefficient (C_T = 0.6). With higher yaw angle, the variation of induction field normal to the disk increases because of the higher skewed angle. In general the Oye's model is again the most accurate momentum model in those cases. The prescribed wake model over-estimates the induction variation considerably at higher yaw angles due to the 'narrower' wake. Note that the prescribed wake model assumes no wake expansion. The vorticity of the prescribed wake vortex model behind the rotor is closer to the disk than the free wake vortex model as shown in figure Fig. 9. Therefore the validity of prescribed vortex approach decreases because of the neglect of wake expansion. The narrower wake also influences the radial velocity parallel to the disk as well as axial induction field, a_x. The axial and radial velocities with higher yaw angle in Fig. 8 depict well the effect of wake expansion. Due to the wake expansion, the vortices in the upwind part simulated by the free wake model is closer to the disk than the prescribed wake model, while the vortices simulated by the free wake model in the downwind part is further than the prescribed wake model. Therefore, the prescribed wake model overestimates the axial velocity in the upwind part and the radial velocity in the downwind part, see Fig. 8. In yawed conditions, it can be concluded that the wake expansion affects the radial velocity significantly, resulting in the change in velocity normal to the disk as shown in Fig. 8.

It is interesting to note that for a yaw angle of 90 degrees, the actuator disk is aligned with incoming velocity where the resultant force acts perpendicular to the disk as a lifting body. Therefore the concept of Glauert's yaw model is still valid as shown in Fig. 7.

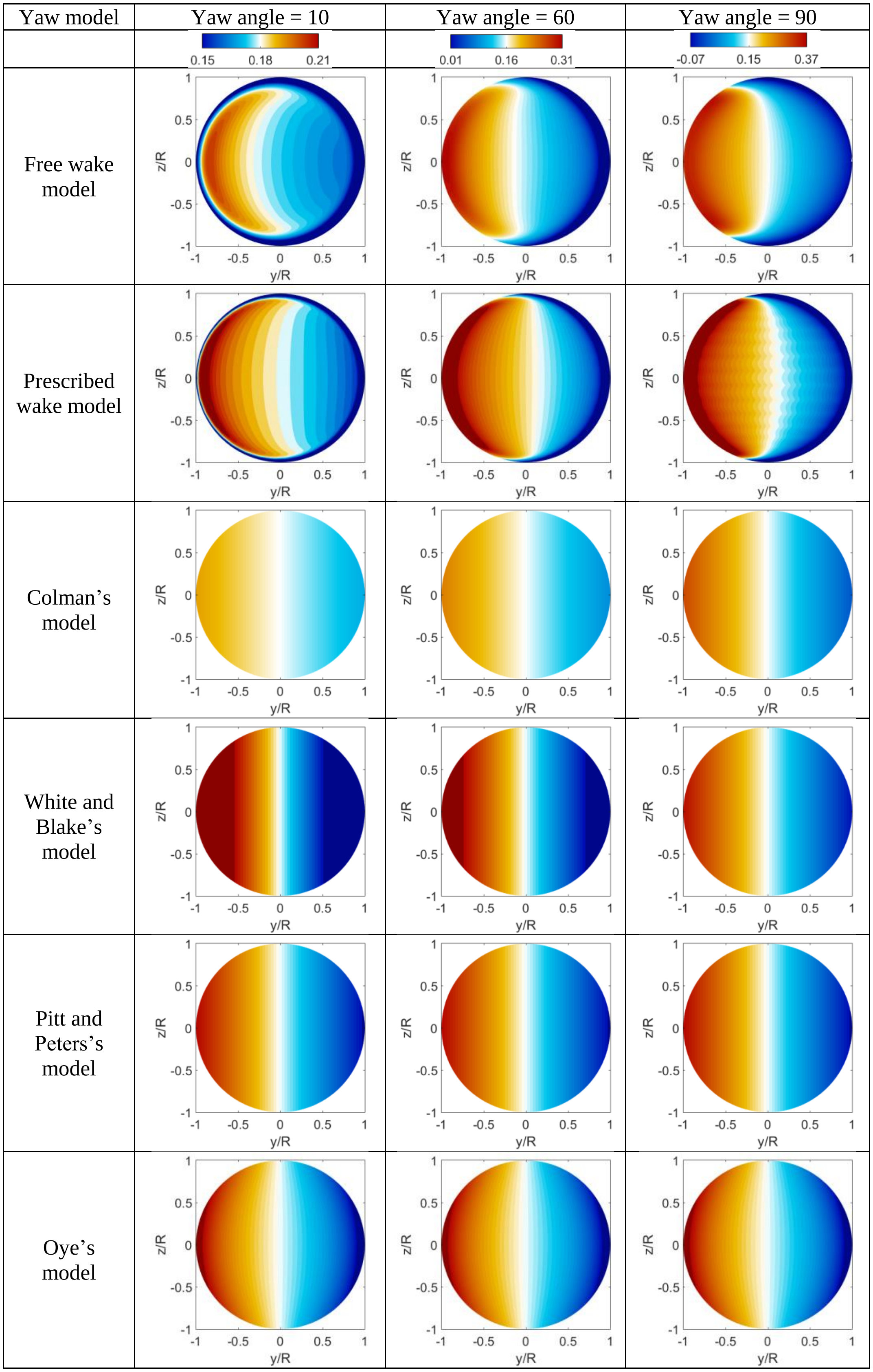

Fig. 7. Induction field (a_n) of CASE III (C_T = 0.6, yaw angle = 10/60/90 deg)

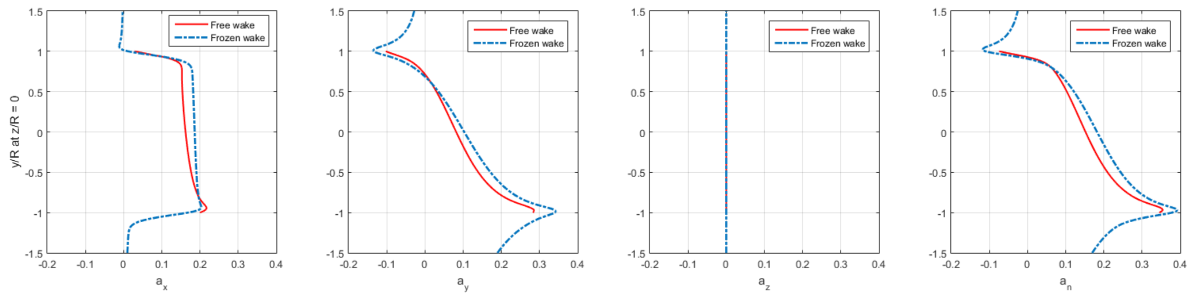

Fig. 8. 3-dimensional induction field (a_x, a_y, a_z) and induction field normal to disk (a_n) (z/R = 0, C_T = 0.6, yaw angle = 60 deg)

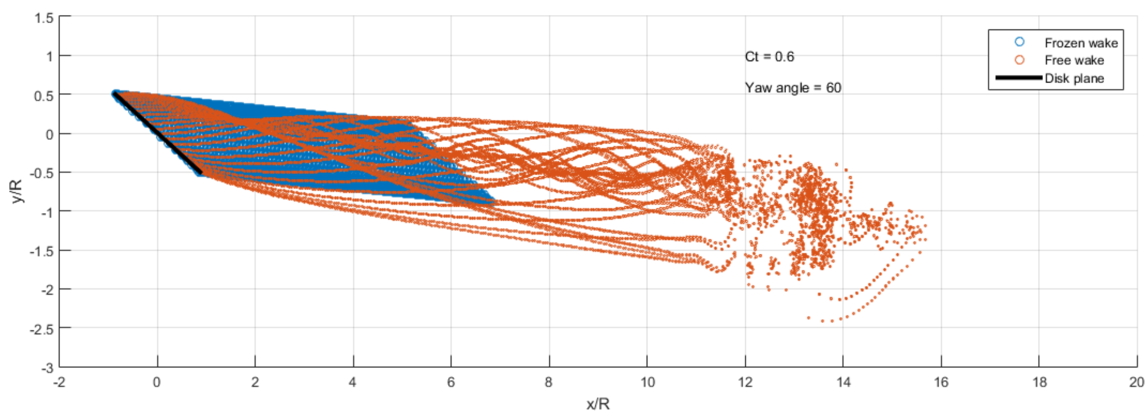

Fig. 9. Top view of wake geometry of vortices simulated by prescribed and free vortex wake models (C_T = 0.6, yaw angle = 60 deg)

4. Case IV: Prediction of C_T and C_p

In momentum theory, C_T can be expressed in terms of a induction factor as in Eq. (1). Fig. 11 shows the calculated C_T based on the induction fields of Fig. 4 (yaw angle = 30 deg and the initial C_T = 0.6). In case of the yaw momentum models and the prescribed wake vortex model, the integral of C_T is 0.59~0.60 as it is assumed, while the C_T of free wake vortex model is 0.575. This indicates that the yaw momentum models and the prescribed wake vortex model predicts higher induction field (approximately 5 %) on the rotor plane. This trend is same as for non-yawed cases, see the Fig. 2. Note that C_T on the rotor plane in Fig. 10 is not uniform which tackles the assumption that the load is uniform on the rotor. Therefore it is important to apply the more accurate load distribution to BEM in yawed conditions.

The maximum power which can be extracted by a yawed actuator disk is calculated in figure Fig. 11. Since it is assumed that the force is normal to the disk, power is the integral of the product of the force normal to the disk and the wind velocity normal to the disk as in Eq. (11).

$$P = \int_V \vec{f} \cdot \vec{U} dV = f_d \cdot U_{i,total} \tag{11}$$

Fig. 11 shows the C_P on the rotor plane. Net C_P of yaw momentum models and the prescribe wake vortex model is approximately 0.491-495, while the C_P of free wake vortex model is 0.499 due to the lower induction field. Generally speaking, power can be abstracted from wind is higher in the upwind part and lower in the downwind part. The two parts counteract each other. Dahlberg's research [26] shows that the power has yaw dependency of wind turbines as in Eq. (12).

$$P = P_0 \cos^x \left(\Phi_y \right) \tag{12}$$

According to his experiment x varies from 1.88 to 5.14. Since the range of x value is wide, the yaw angle dependency of power for an actuator disk is recommended to be studied in detail in the future.

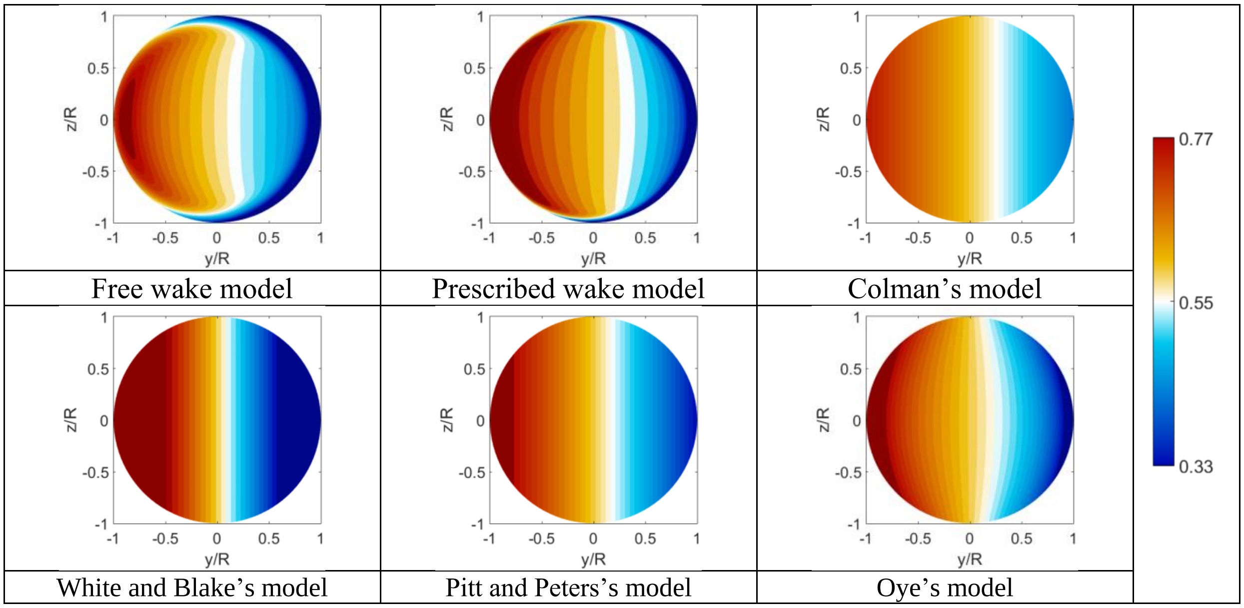

Fig. 10. Thrust coefficient (C_T) for a yawed actuator disk (C_T = 0.6, yaw angle = 30 deg)

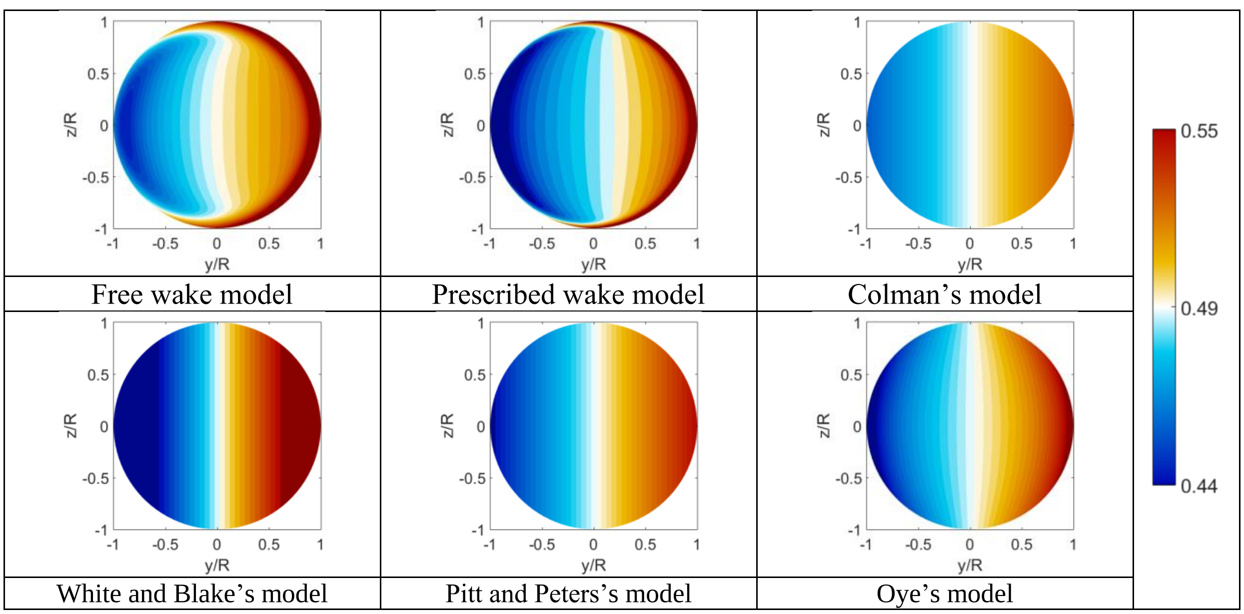

Fig. 11. Maximum power coefficient (C_p) abstracted from a yawed actuator disk (C_T = 0.6, yaw angle = 30 deg)

V. Conclusions

Several momentum models for a uniformly loaded actuator disk in yawed conditions are evaluated by comparing them with higher fidelity models i.e. a prescribed and a free wake vortex ring model, where the last is seen as the highest fidelity model. The assumption of uniform load on the disk causes the creation of vorticity at the disc edge which is then convected downstream. For yawed flow the wake will be deflected due to the lateral force from the disk to inflow, resulting in a skewed wake effects. The induction field normal to the disk is simulated by momentum and vortex models to predict the skewed wake effect at different C_T (0.1 ~ 0.9) and yaw angles (0 ~ 90 degrees).

The accuracy from the momentum models depend on yaw models. White and Blade's correction overestimates the induction field normal to the disk, while Coleman's correction underestimates it. Øye's results agree with the results from the prescribed wake vortex model well, which is probably caused by the fact that Øye's analytical solution is based on a prescribed vortex wake ring model with similar assumptions as the prescribed wake vortex model from the present study. However Øye's model does not predict the wake expansion effects, leading to inaccurate estimation of the radial velocity. At yawed conditions, the radial velocity plays an important contribution to the velocity and loads normal to the rotor plane.

Based on the induction fields estimated by momentum and vortex wake models, the calculated C_T is not uniform, which tackles the assumption that the load is constant on the rotor plane in yawed conditions. Hence, it is important to apply more accurate un-uniform load distribution to BEM in yawed flow.

The extracted power on the disk also has variation from the upwind part oppose those in downwind part. The further research regarding to the yaw angle dependency of power will be performed in the future.

BEM should be improved for yawed conditions where an analytical solution should especially model the radial velocity in a more accurate way.

Finally it is strongly recommended to investigate a highly loaded actuator disk in yawed flow, using a model which includes viscous effects to verify Glauert's empirical correction (See Fig. 3).

References

1. Micallef, D., et al. *Validating BEM, Direct and Inverse Free Wake Models with the MEXICO Experiment*. in *48th AIAA Aerospace Sciences Meeting Including the New Horizons Forum and Aerospace Exposition*. 2010.
2. Ceyhan, J.S.O., et al. *Latest results from the EU project AVATAR: Aerodynamic modelling of 10 MW wind turbines*. in *Journal of Physics: Conference Series*. 2016. IOP Publishing.
3. Rahimi, H., et al. *Investigation of the current yaw engineering models for simulation of wind turbines in BEM and comparison with CFD and experiment*. in *Journal of Physics: Conference Series*. 2016. IOP Publishing.
4. Glauert, H., *A general theory of the autogyro*. Vol. 1111. 1926: HM Stationery Office.
5. Berdowski, T., *Three-Dimensional Free-Wake Vortex Simulations of an Actuator Disc in Yaw and Tilt*, in *2018 Wind Energy Symposium*. 2018, American Institute of Aeronautics and Astronautics.
6. Øye, S. *Induced velocities for rotors in yaw-an extension of the blade element momentum method*. in *Sixth IEA Symposium on the Aerodynamics of Wind Turbines, ECN, Petten*. 1992.
7. Schepers, J.G., *Engineering models in wind energy aerodynamics: Development, implementation and analysis using dedicated aerodynamic measurements.* 2012.
8. Coleman, R.P., A.M. Feingold, and C.W. Stempin, *Evaluation of the induced-velocity field of an idealized helicoptor rotor*. 1945, NATIONAL AERONAUTICS AND SPACE ADMINISTRATION HAMPTON VA LANGLEY RESEARCH CENTER.
9. Pitt, D.M. and D.A. Peters, *Theoretical prediction of dynamic-inflow derivatives.* 1980.
10. White, F. and B.B. Blake. *Improved Method Predicting Helicopter Control Response and Gust Sensitivity*. 1979. American Helicopter Society.
11. Schepers, G. *Avatar: advanced aerodynamic tools of large rotors*. in *33rd Wind Energy Symposium*. 2015.
12. Prandtl, L., *Applications of modern hydrodynamics to aeronautics.* 1923.
13. Burton, T., et el., *Wind Energy Handbook*. 2011: John Wiley & Sons, Ltd.
14. Leishman, G.J., *Principles of helicopter aerodynamics with CD extra*. 2006: Cambridge university press.
15. Micallef, D. and T. Sant, *A Review of Wind Turbine Yaw Aerodynamics*, in *Wind Turbines-Design, Control and Applications*. 2016, InTech.

16. Jiménez, Á., A. Crespo, and E. Migoya, *Application of a LES technique to characterize the wake deflection of a wind turbine in yaw.* Wind energy, 2010. **13**(6): p. 559-572.
17. Joglekar, M. and R. Loewy, *An actuator-disc analysis of helicopter wake geometry and the corresponding blade response*. 1970, ROCHESTER UNIV NY.
18. Schepers, J. *An engineering model for yawed conditions, developed on basis of wind tunnel measurements*. in *37th Aerospace Sciences Meeting and Exhibit*. 1999.
19. Branlard, E., M. Gaunaa, and E. Machefaux. *Investigation of a new model accounting for rotors of finite tip-speed ratio in yaw or tilt*. in *Journal of Physics: Conference Series*. 2014. IOP Publishing.
20. Schmidt, G. and J. Sparenberg, *On the edge singularity of an actuator disk with large constant normal load.* Journal of Ship Research, 1977. **21**(2).
21. Sørensen, J.N., *General momentum theory for horizontal axis wind turbines*. Vol. 4. 2016: Springer.
22. Kuik, G. and L. Lignarolo, *Potential flow solutions for energy extracting actuator disc flows.* Wind Energy, 2016. **19**(8): p. 1391-1406.
23. Glauert, H., *The analysis of experimental results in the windmill brake and vortex ring states of an airscrew*. 1926: HM Stationery Office.
24. Micallef, D., et al., *An investigation of radial velocities for a horizontal axis wind turbine in axial and yawed flows.* Wind Energy, 2013. **16**(4): p. 529-544.
25. Sørensen, J.N. and R. Mikkelsen. *A critical view on the momentum theory*. in *Torque 2012 conference, Oldenburg*. 2012.
26. Dahlberg, J. *Wind Tunnel Measurements of load variations for a yawed turbine with different hub configurations*. in *Proceedings of EWEC Conference*. 1989.